Science World Journal Vol. 19(No 2) 2024 https://dx.doi.org/10.4314/swj.v19i2.19
www.scienceworldjournal.org
ISSN: 1597-6343 (Online), ISSN: 2756-391X (Print)
Published by Faculty of Science, Kaduna State University

Full Length Research Article

EFFECTS OF POST-DEPOSITION ANNEALING ON THE STRUCTURAL AND ELECTRICAL PROPERTIES OF MAGNESIUM-DOPED SB_2S_3 THIN FILMS DEPOSITED BY CHEMICAL BATH DEPOSITION TECHNIQUE

[1]Ele Ugochukwu S., [*2]Nworie Ikechukwu C., [2]A.O. Ojobeagu, [2]P.B. Otah , [3]Mbamara C., [1]P.A. Nwofe and [1]Nwulegu E.N.

[1]Department of Industrial Physics, Ebonyi State University, Abakaliki, Nigeria
[2]Department of Industrial and Medical Physics, David Umahi Federal University of Health Sciences, Uburu, Ebonyi State, Nigeria
[3]Department of Industrial Physics, University of Agriculture and Environmental Science, Umuagwo, Imo State, Nigeria

*Corresponding Author Email Address: nworieikechukwuc@gmail.com

ABSTRACT
In this study, magnesium-alloyed antimony sulfide (Sb_2S_3) thin films were successfully deposited on glass substrates via the chemical bath deposition technique, and the effects of post-deposition annealing on their structural and electrical properties were investigated. The films were grown at room temperature with constant pH, while the magnesium concentrations varied between 0.1M and 0.3M. Post annealing treatment was conducted at temperatures ranging from 100°C to 300°C, with a fixed duration of 1 hour. Characterization of the films was performed using a MiniFlex 600 diffractometer for XRD analysis and UV-spectrophotometer to analyze optical and solid-state properties across the UV-VIS-NIR region. The results demonstrated significant modifications in the structural and optical properties of the films due to the presence of the alloying agent and annealing treatments. X-ray diffraction (XRD) analysis revealed a crystalline orthorhombic structure (PDF#42-1393) for the films, with diffraction peaks corresponding to the stibnite phase, indicating their polycrystalline nature. Higher concentrations of magnesium dopants led to increased intensities of diffraction peaks, reflecting enhanced impurity concentrations, which became more pronounced with increasing annealing temperatures. Optical conductivity curves showed a consistent increase in the extinction coefficient across the wavelength range of 310 nm to 1000 nm for all cases. In as-deposited films, the extinction coefficient (k) uniformly decreased with increasing concentrations of Mg^{2+} ions, ranging from 0.02 to 0.18. However, annealing induced modifications in the extinction coefficient values, with significant reductions observed at higher annealing temperatures. This behavior, reflecting the variation in extinction coefficient with varying Mg^{2+} ion concentrations, suggests potential applications for these films in optoelectronics, photovoltaics, and sensors.

Keywords: Photoconductivity, electrical conductivity, Magnesium, Antimony sulphide, and annealing.

INTRODUCTION

In recent years, there has been a growing interest in exploring the structural and electrical properties of thin films for various technological applications, including photovoltaics, sensors, and optoelectronics. Among the diverse materials investigated for thin film fabrication, antimony sulfide (Sb_2S_3) is a promising candidate due to its favorable optical and electrical characteristics (Barthwal *et al.,* 2022, Farhana *et al.,* 2023, and Ammar *et al.,* 2024). The incorporation of dopants such as magnesium (Mg) in semiconductor thin films especially of Sb_2S_3 thin films offers an avenue for tuning and enhancing their functional properties to meet specific application requirements (Kafizas & Parkin, 2012, Abdelhady *et al.,* 2016 and Priyadarshini et al., 2022). When light is incident on a thin film material, Photoconductivity, an increase in the material's ability to conduct an electric current (electrical conductivity (σ)) occurs (O'Brien *et al.,* 2007), because it generates additional electron-hole pairs, leading to an increase in the density of charge carriers. Consequently, the conductivity of the thin film increases compared to its dark conductivity (The current flowing through a detector when there is no incident photon flux). This phenomenon occurs due to the generation of electron-hole pairs (excitons) within the material when photons are absorbed (Wheeler & Zhang, 2013; Moyez *et al.,* 2016). These excitons can separate under the influence of an electric field, creating free charge carriers (electrons and holes) that contribute to electrical conductivity. Electrical conductivity (σ) is typically influenced by factors such as charge carrier concentration, mobility, and the presence of defects or impurities in the material (Tian *et al.,* 2016). Intrinsic conductivity arises from the movement of free charge carriers (electrons or holes), while extrinsic conductivity can result from dopants or defects introducing additional charge carriers (Jing *et al.,* 2015).
Thin film deposition techniques are categorized into chemical and physical methods, with some techniques incorporating both. Physical deposition includes physical vapor deposition (PVD), sputtering, and plasma techniques, while chemical deposition includes chemical vapor deposition (CVD), spray pyrolysis, and solution growth techniques (SGT). These methods can also be divided into solution deposition (chemical and electrochemical methods) and vapor deposition (chemical and physical vapor methods), each with distinct mechanisms. Chemical vapor transport techniques are used for thin and thick coatings. In chemical deposition, a fluid precursor chemically changes at a substrate, forming a conformal solid layer. Notable chemical methods include spray pyrolysis, solution growth, screen printing, CVD, exchange reactions, electro deposition, anodization, and electrophoresis. Chemical Bath Deposition (CBD), utilized in this study, is popular for its simplicity, reproducibility, convenience, and cost-effectiveness, allowing controlled fabrication of thin films (Min *et al.,* 2020; Christian *et al.,* 2022). The simplicity and scalability of CBD make it particularly attractive for large-scale production of Sb_2S_3 thin films (Christian *et al.,* 2022). For optimizing thin film properties, post-deposition treatments are often required. These

Science World Journal Vol. 19(No 2) 2024 https://dx.doi.org/10.4314/swj.v19i2.19
www.scienceworldjournal.org
ISSN: 1597-6343 (Online), ISSN: 2756-391X (Print)
Published by Faculty of Science, Kaduna State University

treatments enhance the structural and optical characteristics of the films. One such effective method is annealing, which involves heating the films to elevated temperatures in a controlled environment. In this study, the films were annealed at temperatures of 100°C, 200°C, and 300°C, and the effects of these treatments on the optical and structural properties of the films were examined. This process helps in improving film quality by altering its microstructure and reducing defects, leading to enhanced performance (Sun *et al.,* 2017). Annealing has been demonstrated as an effective method for inducing structural transformations, improving crystallinity, and optimizing electrical properties in thin films (Ishiwu *et al.,* 2024).

Nevertheless, the specific effects of annealing on magnesium-doped Sb_2S_3 thin films deposited by CBD remain relatively underexplored; hence, this study investigated the effects of post-deposition annealing on the structural and electrical properties of magnesium-doped Sb_2S_3 thin films deposited via the Chemical Bath Deposition (CBD) technique. The objectives were to analyze structural changes in the films after annealing at 100°C, 200°C, and 300°C, evaluating the impact of annealing on the films' electrical properties, determining the optimal annealing temperature for enhanced performance, and comparing the optical properties of the films before and after annealing to assess improvements in quality and functionality.

MATERIALS AND METHODS

In this experiment, transparent glass slides measuring 75 mm×25 mm×1 mm each were prepared by soaking in hydrochloric acid, acetone, and distilled water to remove contaminants and ensure uniform deposition. 5.7g of $SbCl_3$ was first dissolved in 17 ml of C_3H_6O to which 15.5 ml of 1M $Na_2S_2O_3$ and 100 ml of distilled water were added sequentially and stirred vigorously for 5 minutes by a means of magnetic stirrer. The solution which changed from white to a clear transparent color was poured into different 250 ml beakers labeled A (As-deposited, serving as a control experiment), B (0.1M $MgSO_4$,), C (0.2M $MgSO_4$,) and D(0.3M $MgSO_4$,). Four of the prepared glass substrates were vertically and partially immersed by means of synthetic foams onto each of the four 250 ml beakers. The set up was allowed for 2 hours deposition time after which the substrates were removed from the reacting baths, rinsed with distilled water, hung with clips in open air to dry and labeled accordingly for easy identification. To improve the structural, electrical, and optical properties of the deposited films and activate dopants, the deposited films were annealed at different annealing temperatures, 100˚C, 200˚C and 300˚C at constant annealing time of 60 minutes. The UV spectrophotometer was used for the optical characterization of the films to determine their optical properties, which were then used to infer the electrical properties. The X-ray diffraction (XRD) patterns of the films were obtained using a MiniFlex 600 diffractometer utilizing Cu-Kα radiation with a wavelength (λ) of 1.5406 Å, and the diffraction scans were conducted in the θ-2θ mode over an angular range of 10˚C to 50˚C.

RESULTS AND DISCUSSION

Figure 1 illustrates the XRD patterns of Sb_2S_3 films obtained at various doping concentrations and subsequently annealed at 300 degrees Celsius. The crystalline structure of the Sb_2S_3 thin films was analyzed using XRD technique, with diffraction spectra measured at angle 2θ ranging from 10 to 50 degrees using CuKα radiation (λ=0.15406 nm). The films exhibit a crystalline orthorhombic structure (PDF#42-1393), with all diffraction peaks corresponding to the stibnite phase. The presence of diffraction peaks across all layers indicates that the films are polycrystalline, a finding consistent with previous studies (Ornelas-Acosta *et al.,* 2015).

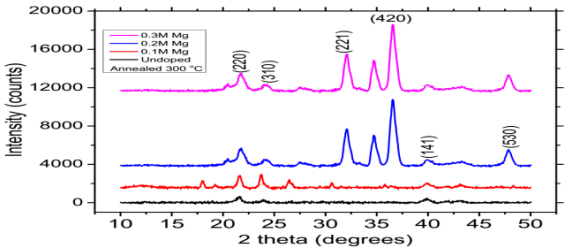

Figure 1: XRD diffractogram of $MgSb_2S_3$ films at different doping concentrations annealed 300˚C

It is evident from the plot that at higher concentrations of dopants, the intensities of the diffraction peaks corresponding to (220), (221), and (420) planes consistently increase, reflecting the augmentation in magnesium impurity concentrations. The patterns show an increase in the sharpness of the peaks as the concentrations of the dopant increase, signifying the growth and enlargement of the crystalline size of the deposited films. This phenomenon arises from the diffusion of magnesium ions within the Sb_2S_3 lattice, facilitating grain growth along new planes.

Science World Journal Vol. 19(No 2) 2024 https://dx.doi.org/10.4314/swj.v19i2.19
www.scienceworldjournal.org
ISSN: 1597-6343 (Online), ISSN: 2756-391X (Print)
Published by Faculty of Science, Kaduna State University

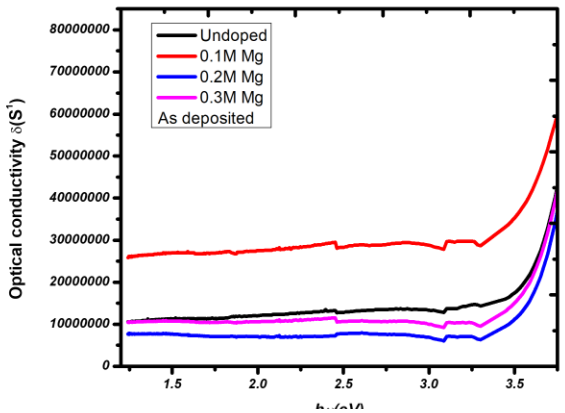

Figure 2: Plot of Optical Conductivity σ_e versus $h\nu$ for as-deposited films

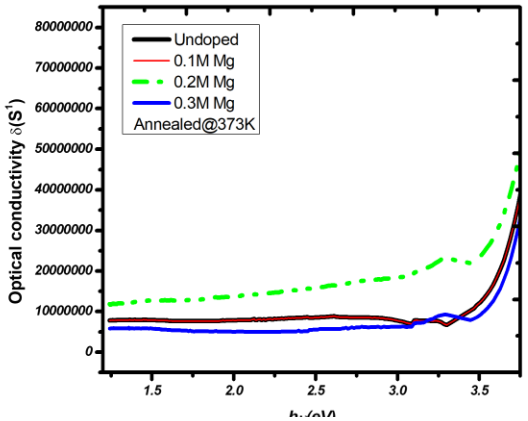

Figure 3: Graph of Optical Conductivity σ_e against $h\nu$ for films annealed at 100˚C

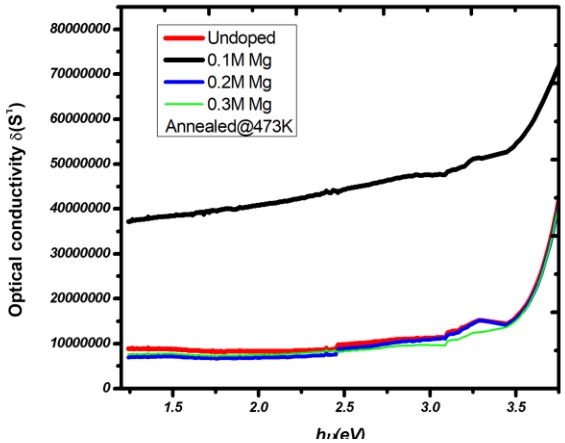

Figure 4: Plot of Optical Conductivity σ_e versus $h\nu$ for films annealed at 200˚C

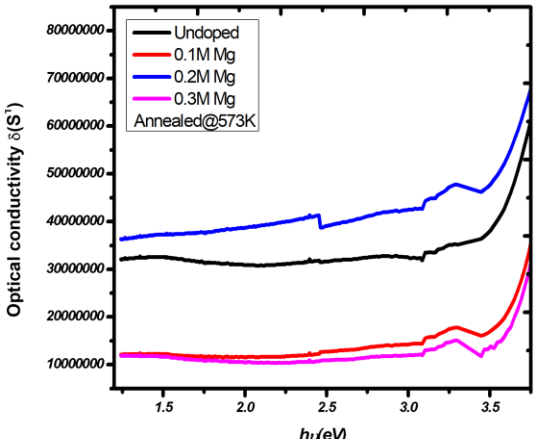

Figure 5: Plot of Optical Conductivity σ_e versus $h\nu$ for films annealed at 300˚C

Science World Journal Vol. 19(No 2) 2024 https://dx.doi.org/10.4314/swj.v19i2.19
www.scienceworldjournal.org
ISSN: 1597-6343 (Online), ISSN: 2756-391X (Print)
Published by Faculty of Science, Kaduna State University

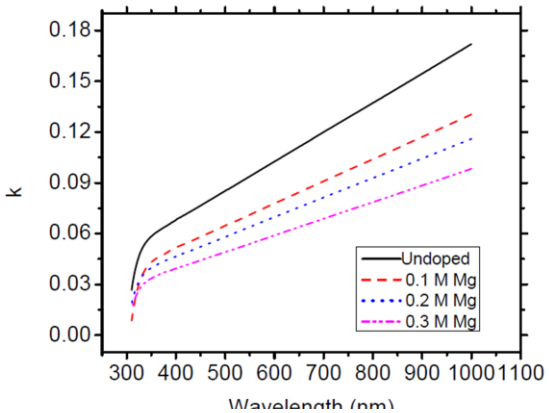

Figure 6: Plot of extinction coefficient k against wavelength for as-deposited films

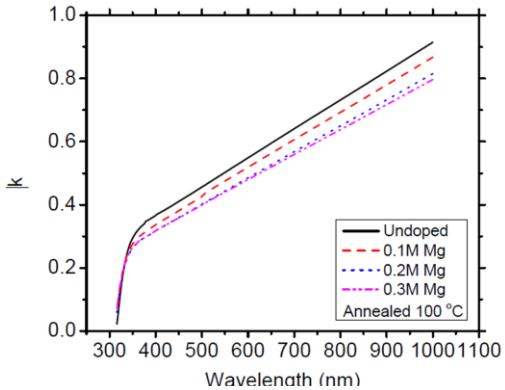

Figure 7: Plot of extinction coefficient k against wavelength for films annealed at 100˚C

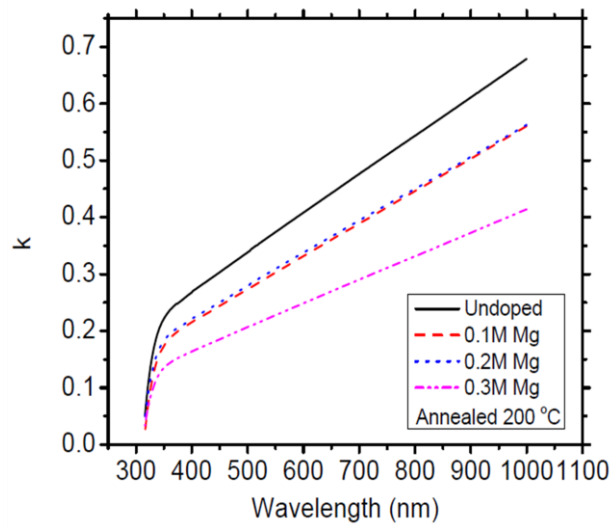

Figure 8: Plot of extinction coefficient k against wavelength for films annealed at 200˚C

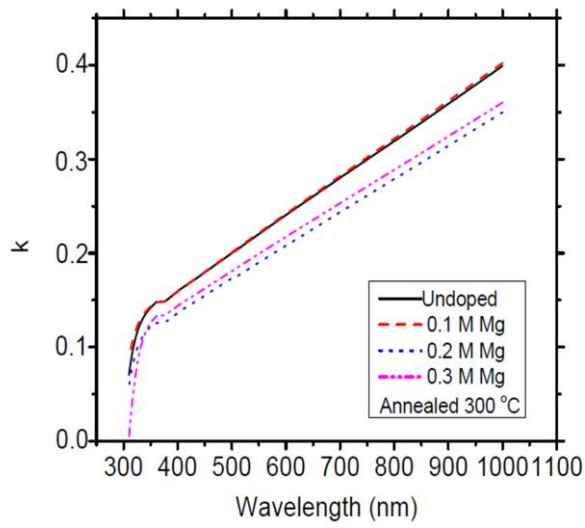

Figure 9: Plot of extinction coefficient k against wavelength for films annealed at 300˚C

Figures 2, 3, 4 and 5 depict the plot of optical conductivity against photon energy for both Sb_2S_3 and Mg-doped-Sb_2S_3 thin films. The optical conductivity exhibited an increase with the rise in photon energy across all films, and was highest between 3.5eV and 3.75eV regardless of annealing conditions. A close look at the figures reveals that optical conductivity varies significantly with Mg concentration and annealing temperature. In As-Grown Films in figure 2, there is a Substantial enhancement, decrease, and slight recovery in optical conductivity of the 0.1M, 0.2M and 0.3M Mg-doped films respectively. This could suggest that Moderate doping (0.1M) improves conductivity, while higher concentrations do not due to dopant saturation or defect states. Optimal doping levels and annealing temperatures enhance conductivity by increasing carrier concentration and reducing defect states (Zhang *et al.,* 2018).

For Films annealed at 100°C as displayed in figure 3, the Undoped & 0.1M Mg-doped films Overlapped at 3.75 eV. The 0.2M Mg-dopped film had a notable increase while the 0.3M Mg-dopped film

decline in conductivity. This implies that annealing at 100°C enhances conductivity for 0.2M Mg-doped films, while higher doping (0.3M) reduces performance due to defect introduction. Figure 4 shows the films annealed at 200°C. The film doped with 0.3M of Mg is similar in conductivity to the undoped film. While the 0.1M Mg-dopped film had a significant increase in conductivity, that of 0.2M was lower. These suggest that at 200°C, 0.1M Mg doping greatly enhances conductivity, but higher levels do not, indicating convergence at higher photon energies. As displayed in figure 5, 0.1M and 0.3M Mg-dopped films annealed at 300°C a decrease in conductivity while that of 0.2M had its conductivity increased. At 300°C, 0.2M Mg doping optimizes conductivity, while 0.1M and 0.3M levels do not, likely due to defect introduction at these concentrations. The maximum optical conductivity is observed for films with 0.1M Mg doping annealed at 200°C.

The extinction coefficient, a fundamental parameter describing a material's light absorption efficiency, was calculated using Equation (1):

$$\alpha = \frac{4\pi k}{\lambda} \qquad 1$$

Here, λ represents the wavelength of incident light, and α denotes the absorption coefficient. Figures 6, 7, 8, and 9 present the plots of extinction coefficient (k) versus wavelength. These plots reveal a uniform increase in the extinction coefficient across the wavelength range of 310 nm to 1000 nm for all cases. This observed trend aligns with observation of (Shaji *et al.,* 2017) as documented in the literature. In the case of as-deposited films, the extinction coefficient (k) uniformly decreased with increasing concentrations of Mg2+ ions, with values ranging from 0.02 to 0.18, as illustrated in Figure 6. However, annealing treatments induced modifications in the extinction coefficient values for both undoped and doped films. Specifically, for annealed films, the values ranged from 0.02 to 0.86 for those annealed at 100°C, 0.025 to 0.7 for those annealed at 200°C, and 0.001 to 0.4 for those annealed at 300°C, as depicted in Figures 7, 8, and 9, respectively. Remarkably, there is a decrease in the extinction coefficient value as the annealing temperature increases. This observed behavior, reflecting the variation of extinction coefficient with varying Mg2+ ion concentrations, is consistent with findings reported by other research groups in the literature (Cifuentes *et al.,* 2006; Ismail *et al.,* 2014 and Garcia *et al.,* 2016). Lower extinction coefficient at higher annealing temperatures suggests improved film quality with fewer defects or impurities, leading to less light absorption.

Conclusion

The examination of the effects of Post-deposition annealing on the structural and electrical Properties of Magnesium-Doped Sb_2S_3 Thin Films has been carried out. The result revealed that Mg doping and annealing temperatures significantly impact the optical (and consequently electrical) conductivity of Sb_2S_3 thin films. Optimal doping concentration and annealing conditions are crucial for maximizing conductivity, with 0.1M Mg doping generally enhancing performance at lower annealing temperatures, while 0.2M Mg doping is more effective at higher temperatures. Higher doping levels tend to introduce defects, reducing conductivity. The Optical conductivity of the films consistently increases with photon energy, suggesting efficient light absorption capabilities, while the extinction coefficient uniformly decreases with increasing Mg2+ ion concentrations in as-deposited films and exhibits a significant reduction with higher annealing temperatures. XRD analysis reveals that Sb_2S_3 thin films, regardless of doping concentration and annealing temperature, exhibit a polycrystalline orthorhombic structure characteristic of the stibnite phase. Higher concentrations of magnesium dopants lead to intensified diffraction peak intensities, indicating enhanced impurity concentrations and crystalline growth, a trend that becomes more pronounced with annealing within the Sb2S3 lattice. Consequently, these films hold promise for applications across various fields, including optoelectronics, photovoltaics, and sensors.

Conflict of Interest

The authors of this work have no conflicts of interest at this time.

Data Availability Statement

The data that support the findings of this study are available from the corresponding author upon reasonable request.

REFERNCES:

Abdelhady, A. L., Saidaminov, M. I., Murali, B., Adinolfi, V., Voznyy, O., Katsiev, K., & Bakr, O. M. (2016). Heterovalent dopant incorporation for bandgap and type engineering of perovskite crystals. *The journal of physical chemistry letters, 7(2), 295-301.* https://pubs.acs.org/doi/abs/10.1021/acs.jpclett.5b02681

Ammar, A. H., El-Sayed, H. E. A., Ali, H. A. M., Salem, G. F., & Moqbel, M. S. (2024). Exploring the optical and photovoltaic characteristics of thermally deposited and annealed antimony sulfide thin films: A comprehensive study. *Optical Materials, 148, 114902.* https://doi.org/10.1016/j.optmat.2024.114902

Barthwal, S., Kumar, R., & Pathak, S. (2022). Present status and future perspective of antimony chalcogenide (Sb_2X_3) photovoltaics. *ACS Applied Energy Materials, 5(6), 6545-6585.* https://doi.org/10.1021/acsaem.2c00420

Christian, N. I., Ekuma, A. P., & Osondu, N. (2022). Phytochemical, Optical and FTIR Studies of ZnSe Thin Films for Solar Energy Applications. IOSR Journal of Applied Physics (IOSR-JAP), 14(01), pp. 25-29. https://www.iosrjournals.org/iosr-jap/pages/v14(1)Series-3.html

Cifuentes, C., Botero, M., Romero, E., Calderon, C., and Gordillo, G. (2006). Optical and structural studies on SnS Films Grown by Co-evaporation. *Brazilian Journal of Physics*, *36*(3B), 1046-1049. https://doi.org/10.1590/S0103-97332006000600066

Farhana, M. A., Manjceevan, A., & Bandara, J. (2023). Recent advances and new research trends in Sb_2S_3 thin film based solar cells. *Journal of Science: Advanced Materials and Devices, 8(1), 100533.* https://doi.org/10.1016/j.jsamd.2023.100533

Garcia, R. A., Avendaño, C. M., Pal, M., Delgado, F. P., and Mathews, N. R. (2016). Antimony sulfide (Sb_2S_3) Thin Films by Pulse Electrodeposition: Effect of Thermal Treatment on Structural, Optical and Electrical Properties. *Materials Science in Semiconductor Processing*, *44*, 91-100. https://doi.org/10.1016/j.mssp.2015.12.018

ISHIWU, S., NWORIE, I., AGBO, P., OJOBEAGU, A., OTAH, P., &

ELEKWA, C. (2024). Distinguishing Traits Of Thin Films Of Antimony-Doped Cadmium Selenide (Cdse/Sb) On Glass Substrate Versus Fluorine Tin Oxide (Fto) Through Spray Pyrolysis: An Investigative Analysis. Global Journal of Pure and Applied Sciences, 30(1), 115-118. https://www.ajol.info/index.php/gjpas/article/view/267570

Ismail, B., Mushtaq, S., Khan, R. A., Khan, A. M., Zeb, A., and Khan, A. R. (2014). Enhanced Grain Growth and Improved Optical Properties of the Sn doped Thin Films of Sb_2S_3 Orthorhombic Phase. *Optik-International Journal for Light and Electron Optics*, *125*(21), 6418-6421. https://doi.org/10.1016/j.ijleo.2014.06.138

Jing, T., Dai, Y., Ma, X., Wei, W., & Huang, B. (2015). Effects of intrinsic defects and extrinsic doping on the electronic and photocatalytic properties of Ta 3 N 5. *RSC advances, 5(73), 59390-59397.* https://doi.org/10.1039/C5RA08563B

Kafizas, A., & Parkin, I. P. (2012). Inorganic thin-film combinatorial studies for rapidly optimising functional properties. *Chemical Society Reviews, 41(2), 738-781.* https://doi.org/10.1039/C1CS15178A

Min, H. S., Saha, D., Kalita, J. M., Sarma, M. P., Mukherjee, A., Ezekoye, B., & Pathak, T. K. (2020). Nanostructure Thin Films: Synthesis and Different Applications. *In Functionalized Nanomaterials I (pp. 71-82). CRC Press.*

Moyez, A., Dhar, A., Sarkar, P., Jung, H. S., & Roy, S. (2016). A review of the multiple exciton generation in photovoltaics. *Reviews in Advanced Sciences and Engineering, 5(1), 51-64.*

O'Brien, P. G., Kherani, N. P., Zukotynski, S., Ozin, G. A., Vekris, E., Tetreault, N., & Miguez, H. (2007). Enhanced Photoconductivity in Thin-Film Semiconductors Optically Coupled to Photonic Crystals. *Advanced Materials, 19(23), 4177-4182.* https://doi.org/10.1002/adma.200700564

Ornelas-Acosta, R. E., Shaji, S., Avellaneda, D., Castillo, G. A., Roy, T. D., & Krishnan, B. (2015). Thin Films of Copper Antimony Sulfide: a Photovoltaic Absorber Material. *Materials Research Bulletin*, *61*, 215-225 https://doi.org/10.1016/j.materresbull.2014.10.027

Priyadarshini, P., Das, S., & Naik, R. (2022). A review on metal-doped chalcogenide films and their effect on various optoelectronic properties for different applications. *RSC advances, 12(16), 9599-9620.* https://doi.org/10.1039/D2RA00771A

Shaji, S., Garcia, L. V., Loredo, S. L., Krishnan, B., Martinez, J. A., Roy, T. D., and Avellaneda, D. A. (2017). Antimony SulphideThin Films Prepared by Laser Assisted Chemical Bath Deposition. *Applied Surface Science,* 393, 369-376.

Sun, Q., Fassl, P., Becker-Koch, D., Bausch, A., Rivkin, B., Bai, S., & Vaynzof, Y. (2017). Role of microstructure in oxygen induced photodegradation of methylammonium lead triiodide perovskite films. Advanced Energy Materials, 7(20), 1700977. https://doi.org/10.1002/aenm.201700977

Tian, T., Cheng, L., Zheng, L., Xing, J., Gu, H., Bernik, S., & Li, G. (2016). Defect engineering for a markedly increased electrical conductivity and power factor in doped ZnO ceramic. *Acta Materialia, 119, 136-144.* https://doi.org/10.1016/j.actamat.2016.08.026

Wheeler, D. A., & Zhang, J. Z. (2013). Exciton dynamics in semiconductor nanocrystals. *Advanced Materials, 25(21), 2878-2896.* https://doi.org/10.1002/adma.201300362

Zhang, Q., Song, Q., Wang, X., Sun, J., Zhu, Q., Dahal, K., & Ren, Z. (2018). Deep defect level engineering: a strategy of optimizing the carrier concentration for high thermoelectric performance. Energy & Environmental Science, 11(4), 933-940. https://doi.org/10.1039/C8EE00112J